3D MONTE CARLO RADIATIVE TRANSFER IN INHOMOGENEOUS STELLAR WINDS
APPLICATION TO RESONANCE LINE FORMATION

Astronomický ústav AV ČR

Brankica Kubátová[1]
brankica.kubatova@asu.cas.cz

W.-R. Hamann[2], **J. Kubát**[1], **L. M. Oskinova**[2]

[1]Astronomický ústav, Akademie věd České republiky, CZ-251 65 Ondřejov, Czech Republic

[2]Institut für Physik und Astronomie, Universität Potsdam, 14476 Potsdam-Golm, Germany

ABSTRACT

The instability of wind radiative driving may cause the occurrence of wind shocks and spatial wind density and velocity structures i.e. clumps. Observational evidence suggests that clumpy structures are a common property and a universal phenomenon of all massive, hot star winds. The structured stellar winds are essentially three-dimensional (3D), and the full description requires the 3D radiative transfer. In this poster a full 3D Monte Carlo radiative transfer code for inhomogeneous expanding stellar winds is presented. We show how different model parameters influence resonance line formation. By modeling UV resonance lines, we demonstrate how wind inhomogeneities may influence line profiles.

WIND MODEL

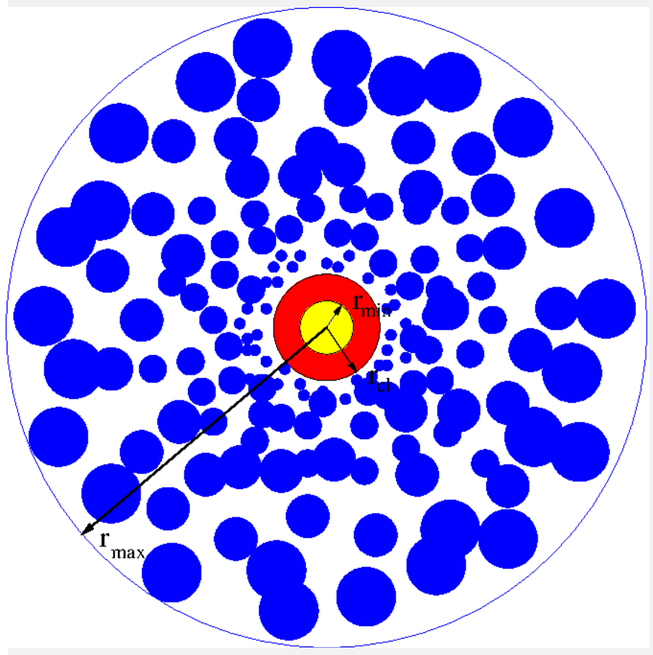

- **SMOOTH** region $r_{\rm min} < r < r_{\rm cl}$
  One density component
  $r_{\rm min} = R_*$; $r_{\rm cl}$ – onset of clumping
- **CLUMPED** region $r_{\rm cl} < r < r_{\rm max}$
  Two density components:
  INTER-CLUMP MEDIUM (ICM)
  CLUMPS
- Underlying wind velocity

$$v_\beta(r) = v_\infty \left(1 - \frac{b}{r}\right)^\beta$$

- Wind opacity (Hamann, 1980)

$$\chi(r) = \frac{\chi_0}{r^2 v_\beta(r)/v_D}\, q(r)\, \phi_x$$

$$\phi_x = \frac{1}{\sqrt{\pi}}\, e^{-x^2}$$

- χ_0 – opacity parameter; x – dimensionless frequency; $q(r) \equiv 1$ (constant ionization condition)

DESCRIPTION OF CLUMPING

- Macro-clumping – clumps can be optically thin or thick
- Clumps are statistically distributed with average separation $L = L(r)$
- Clumps are assumed to be spherical with the radius $l = l(r)$
- Density in clumps $\rho_{\rm cl}(r) = D\,\rho_{\rm sw}(r)$; $D \geqslant 1$ – clumping factor
- For void ICM, the volume filing factor is $f_V = 1/D \quad \Rightarrow$

$$D = \frac{L^3(r)}{\frac{4\pi}{3} l^3(r)}$$

- Number density of clumps $n_{\rm cl} \propto \frac{1}{r^2 v_r} \Rightarrow L = n_{\rm cl}^{-1/3}$; L_0 – the clump separation parameter

$$L(r) = L_0 \sqrt[3]{r^2 \frac{v_r}{v_\infty}} \qquad l(r) = l_0 \sqrt[3]{r^2 \frac{v_r}{v_\infty}}$$

- The density of ICM, $\rho_{\rm ic} = d\,\rho_{\rm sw}$; $\quad 0 \leqslant d < 1$ – ICM density factor
- For the case of dense clumps and non-void ICM $\Rightarrow f_V = (1-d)/(D-d)$
- The distance r_i of the i-th clump from the stellar center
  $r_i = (r_{\rm max} - r_{\rm cl})\xi_i + r_{\rm cl}$; $\quad i = 1, N_{\rm cl}$; $\quad 0 < \xi_i \leqslant 1$ – random number; $N_{\rm cl}$ – total number of clumps
- $1/v_\beta(r)$ – probability density distribution function
- Velocity inside clumps ($v_{\rm dis} = m\,v_\beta(r)$, $0 < m \leqslant 1$; $r_i^{\rm c}$ – position of the i-th clump's ceter)

$$v(r) = v_\beta(r) + v_{\rm dis}\, \frac{r - r_i^{\rm c}}{l_i}$$

- **ASSUMPTIONS:** lower boundary - line-free continuum and no limb darkening; only scattering lines; complete redistribution; pure Doppler-broadening

SCHEME OF THE CODE

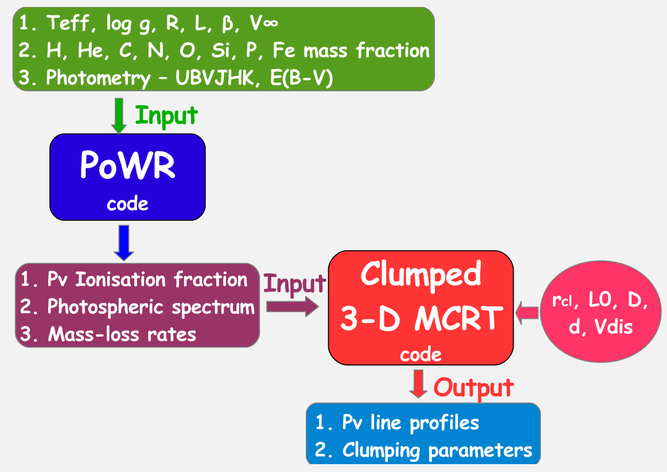

The observed spectra are simulated with Potsdam Wolf-Rayet (**PoWR**) non-LTE model atmospheres code. The mass-loss rates are adjusted to fit to the observed Hα emission lines best. For the unsaturated UV resonance lines (e.g., P v) we then applied our 3D Monte-Carlo code, which can account for wind clumps of any optical depths ("macro-clumping"), a non-void inter-clump medium, and a velocity dispersion inside the clumps. The ionization stratifications and underlying photospheric spectra are adopted from the **PoWR** models. The properties of wind clumps are constrained by fitting the observed resonance line profiles.

COMPARISON WITH OBSERVATION

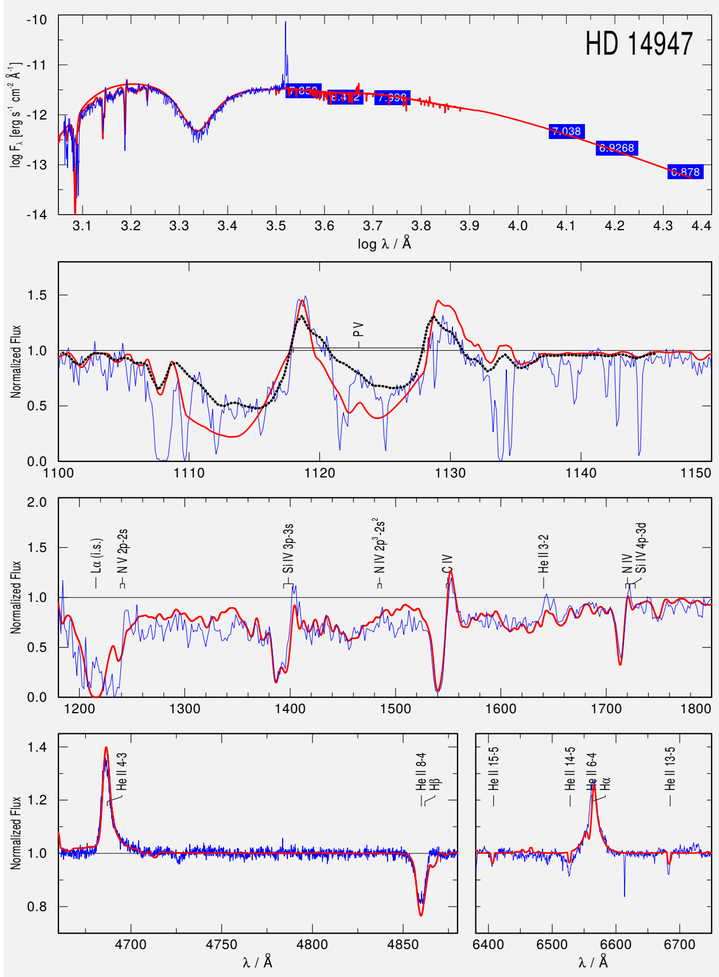

Figure: Best fit from **PoWR** modeling (thick red solid lines) to the observed HD 14947 spectra (thin blue solid lines), together with the calculated P v line profile from 3D Monte-Carlo code (black dotted line).
Blue labels with numbers in the upper panels are UBVJHK magnitudes. The spectral region of the P v resonance doublet was covered by high-resolution observations with FUSE, which we retrieved from the MAST archive. Low-resolution near-ultraviolet (NUV) spectra (1200 to 2000 Å), taken with the IUE, were downloaded from the INES Archive Data Server. Optical spectra were taken with a CCD SITe ST-005 800 2000 pix cam-era attached to the Coudé spectrograph of the 2-m telescope at the Ondřejov Observatory in Czech Republic (Šurlan et al., 2013).

Table: Clumping parameters that give the best fit to the observed P v line profiles.
Adjusted wind parameters are
$\dot{M} = 2.82 \cdot 10^{-6}\, M_\odot/yr$ and $v_\infty = 2350\ km/s$.

Star	L_0	$r_{\rm cl}$	d	D	$v/v_{\rm dis}$
HD 14947	0.5	1 $[R_*]$	0.2	10	0.1

UV RESONANCE LINE PROFILES

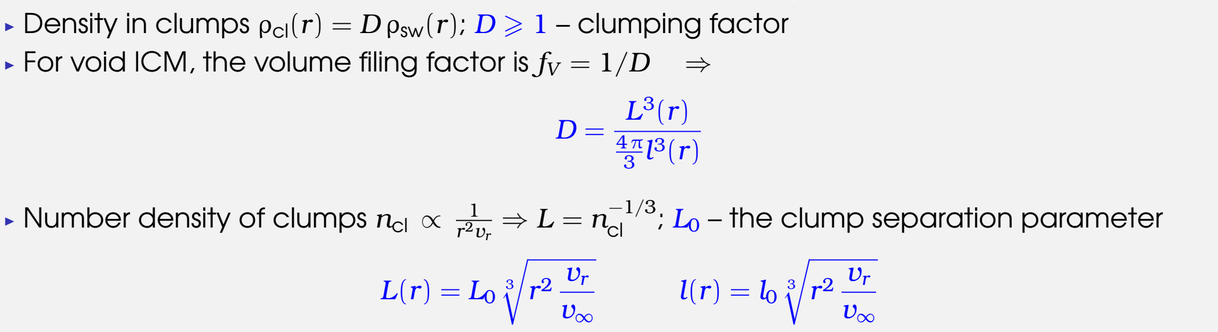

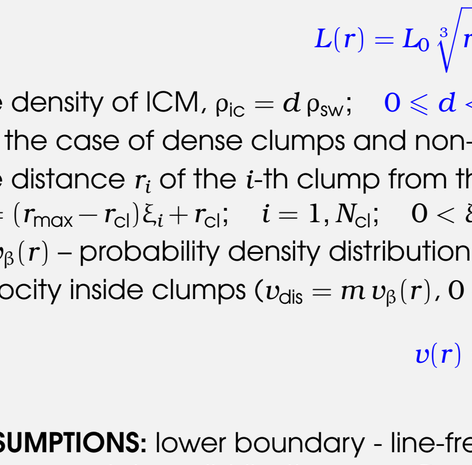

Figure: Line profiles for weak (upper left panel), medium (upper midle panel), and strong (upper right panel) lines for different number of clumps distribution (as example see lower panel). Black lines correspond to smooth models; other colored lines correspond to clumped models with different number of clumps (Šurlan et al., 2012).

CONCLUSIONS

- When macroclumping is taken into account line strength becomes significantly weaker.
- For given D, the key model parameter L_0 affecting the effective opacity.
- Onset of clumping $r_{\rm cl}$ affects the line shape; absorption dip near the line center may provide an effective diagnostic tool for the onset of clumping.
- The line saturation is strongly affected by the ICM.
- Increasing the velocity dispersion inside clumps $\Rightarrow$ the absorption extends to higher velocities than v_∞.
- In case of resonance doublets, clumping effects are analogous to the case of single lines.
- Our 3D model confirms that any mass-loss diagnostics which do not account for wind clumping must underestimate the actual $\dot{M}$.
- Macro-clumping resolves the previously reported discrepancy between Hα and P v mass-loss diagnostics.

REFERENCES

Hamann, W.-R. 1980, A&A, 84, 342
Šurlan, B., Hamann, W.-R., Kubát, J., Oskinova, L., Feldmeier, A., 2012, A&A, 541, A37
Šurlan, B., Hamann, W.-R., Aret, A., Kubát, J., Oskinova, L., Torres, A. F., 2013, A&A, 559, A130

ACKNOWLEDGEMENTS

This work has been supported by GA ČR grant 16-01116S.